Ultrasonic investigation of amorphous superconducting films

J. Schmidt* and M. Levy
Department of Physics, University of Wisconsin–Milwaukee, Milwaukee, Wisconsin 53201

A. F. Hebard
AT&T Bell Laboratories, Murray Hill, New Jersey 07974
(Received 2 February 1994)

Measurements of the surface-acoustic-wave (SAW) attenuation and dc resistance of several amorphous superconducting In/InO_x films as a function of temperature exhibit an excess SAW attenuation below the Kosterlitz-Thouless transition temperature, which cannot be accounted for by the presence of flux-flow resistance due to unbound vortices in these films. Qualitative agreement with the observed SAW attenuation below the Kosterlitz-Thouless temperature may be obtained by using a model based on the attenuation produced by bound vortex pairs present in the films below the Kosterlitz-Thouless transition temperature.

INTRODUCTION

In 1973, Kosterlitz and Thouless[1] proposed that a topological phase transition should occur in two-dimensional systems containing "topological defects" whose interaction energy has a logarithmic dependence on separation. Beasley, Mooij, and Orlando[2] were able to show that such a transition should occur in a superconducting film with large normal-state sheet resistance. In such films the topological defects are thermally excited magnetic vortices. Below a certain temperature T_c (usually referred to as the Kosterlitz-Thouless transition temperature) the magnetic vortices will be bound in pairs and will produce no dissipation in the flow of an applied current. At T_c, the vortex pairs begin to unbind and produce a flux-flow resistance. Thus, the Kosterlitz-Thouless transition should make itself evident in the resistive transition and the current-voltage relations in these films.

Evidence for the existence of the Kosterlitz-Thouless transition has been found primarily in amorphous superconducting films. Broadening of the resistive transitions in amorphous In/InO_x films has been reported[3] to be in agreement with the predictions of the Kosterlitz-Thouless theory. Further evidence for the existence of the Kosterlitz-Thouless transition has been observed in the current-voltage measurements made on amorphous HgXe films[4–6] and on amorphous In/InO_x films,[7] as well as in the measurements of the complex ac impedance made by Hebard and Fiory.[8] The bulk of the investigation into the Kosterlitz-Thouless transition has been restricted to studies of the resistance and current-voltage characteristics of these films. Another independent verification of the Kosterlitz-Thouless transition would be desirable. Therefore, it was decided to look at the behavior of the attenuation of surface-acoustic waves (SAW's) in amorphous In/InO_x films.

EXPERIMENTAL DATA

Data on the dc resistance and SAW attenuation were obtained on five amorphous In/InO_x films. The films studied in the investigation were produced by reactive ion-beam sputter deposition onto a y-z $LiNbO_4$ substrate in an argon-oxygen atmosphere. The details of the deposition process have been described in a previous work.[9] The techniques for measuring the dc resistance and SAW attenuation have also been presented in a previous work.[10]

The normalized dc resistance and SAW attenuation data for the five films are shown in Figs. 1–5. The normal-state sheet resistance (R_n), the mean-field superconducting transition temperature (T_{c0}), the Kosterlitz-

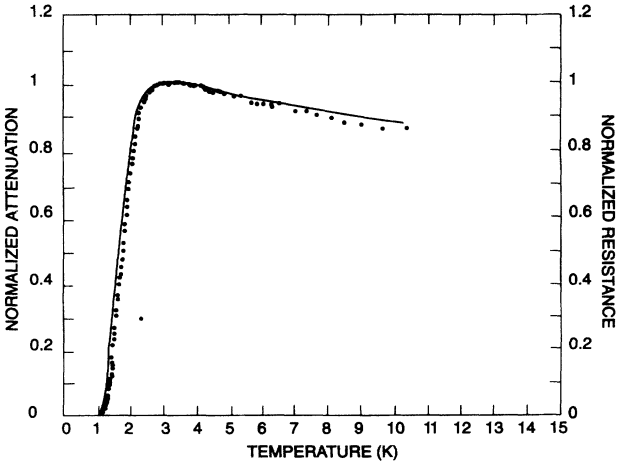

FIG. 1. Normalized resistance data (solid curve) and normalized SAW attenuation data (points) for sample *A*.

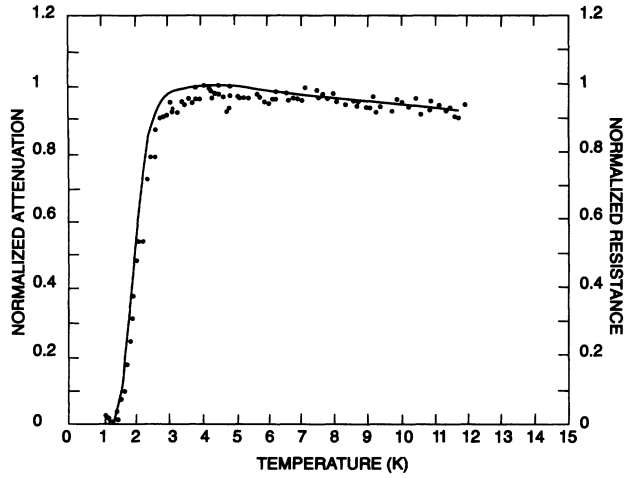

FIG. 2. Normalized resistance data (solid curve) and normalized SAW attenuation data (points) for sample *B*.

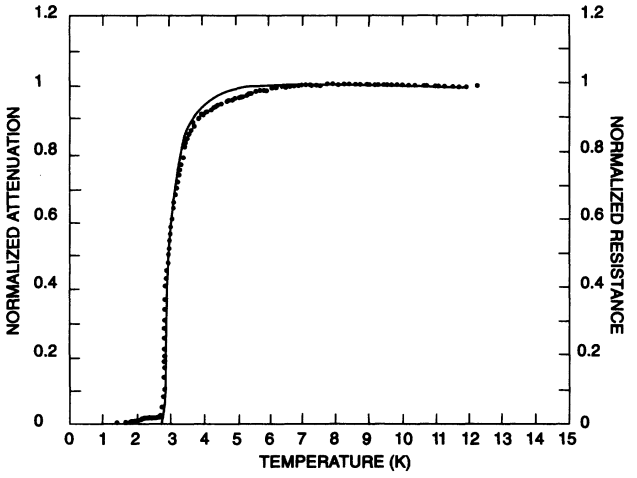

FIG. 3. Normalized resistance data (solid curve) and normalized SAW attenuation data (points) for sample *C*.

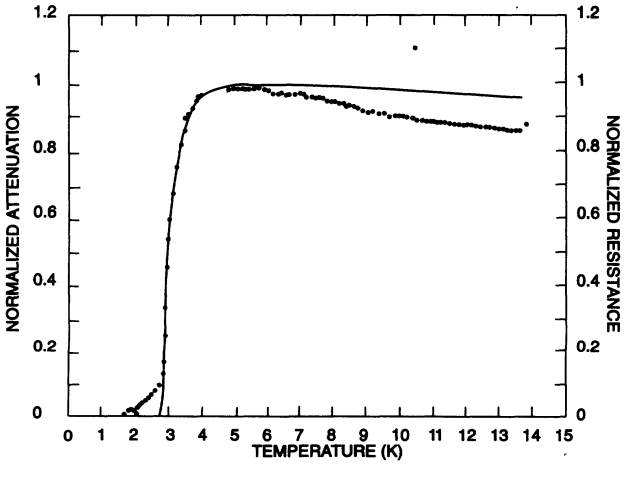

FIG. 4. Normalized resistance data (solid curve) and normalized SAW attenuation data (points) for sample *D*.

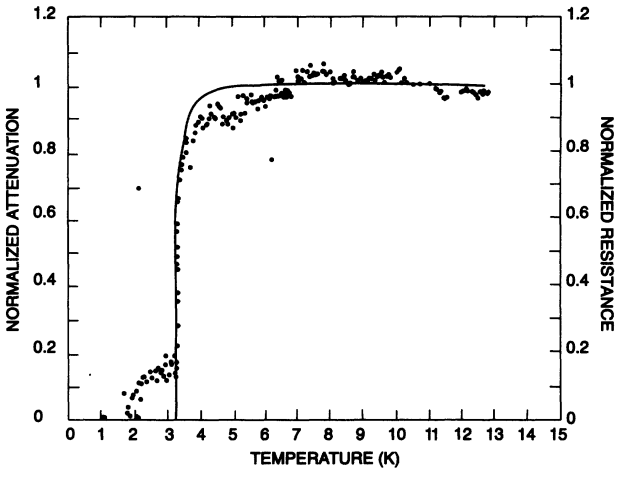

FIG. 5. Normalized resistance data (solid curve) and normalized SAW attenuation data (points) for sample *E*.

Thouless transition temperature (T_c), defined as the temperature at which the film resistance fell below 10^{-7} of the normal-state resistance, the measured normal-state attenuation (α_n) and the predicted acoustoelectric attenuation (α_{ac}) for each of the samples are listed in Table I. The values of R_n and T_{c0} for each of the films were determined by fitting the resistance data to the Aslamosov-Larkin paraconductivity theory[11] in the region where the temperature coefficient of resistance is positive. The measured attenuation, with the exception of sample *E*, was taken to be the maximum attenuation in the normal state. For sample *E*, the normal-state attenuation was given by the y intercept of the straight line fit to the attenuation above T_{c0}.

The absorption of SAW energy in the normal state is produced by acoustoelectric coupling of the SAW polarization field in the piezoelectric substrate to the sheet resistivity of the deposited film. The attenuation decrease between the normal and the superconducting states is caused by superconducting quenching of this acoustoelectric effect.[12] The acoustoelectric attenuation was calculated using the results of the work by Ingebrigtsen and Adler[13–15]

$$\alpha_{ae}=\frac{\omega K^2}{2}(\epsilon_p+\epsilon_0)R_n \ . \tag{1}$$

In Eq. (1), ω is the angular frequency of the SAW, K is the piezoelectric coupling constant of the $LiNbO_3$ substrate, and $\epsilon_p(\epsilon_0)$ is the dielectric constant of the substrate (vacuum). The frequency of the SAW used in this investigation was 680 MHz.

In Figs. 1–5 we see that for samples *A* and *B*, the normalized attenuation and normalized resistance curves coincide with one another. However, for the other samples we notice a distinct "foot" in the attenuation data. We believe that this foot is due to the presence of bound vortex pairs in the film. We shall discuss this aspect of the data in the next section.

TABLE I. Data obtained on the In/InO_x samples used in this investigation.

Sample	R_n ($\Omega/\square$)	T_{c0} (K)	T_c (K)	T_c/T_{c0}	α_n (dB/cm)	α_{ac} (dB/cm)	Film thickness (Å)
A	8041	2.79	1.2	0.43	13.43	17.18	100
B	4594	3.27	1.5	0.45	10.51	11.44	100
C	2660	3.19	2.8	0.88	5.97	6.47	100
D	1643	3.33	2.8	0.84	6.54	6.57	100
E	340	3.24	3.24	1.00	0.92	0.84	400

DISCUSSION—AMORPHOUS In/InO_x FILMS

The characteristics of the five amorphous In/InO_x films are summarized in Table I. Although our focus is on the SAW attenuation in these films, there are a few observations that will be made concerning the resistance data. As the normal-state sheet resistance increases, both T_c and T_{c0} tend to decrease. The decrease in T_{c0} with increasing normal-state sheet resistance has been observed for other amorphous In/InO_x films.[9]

The universality prediction of Minnhagen[16] may also be tested for the amorphous In/InO_x films. According to Minnhagen if $\ln(R/R_n)$ is plotted as a function of the parameter X, defined by

$$X=\left[\frac{T}{T_{c0}-T}\right]\left[\frac{T_{c0}-T_c}{T_c}\right], \tag{2}$$

the result should be a universal curve. We have done this for our films and the results are shown in Fig. 6. As may be seen in the region where the resistance drops sharply, it appears that the universality prediction of Minnhagen holds for these films.

Let us now turn our attention to the SAW attenuation data. There are several interesting features that should be pointed out. First, we see that the normal-state attenuation is very close to the predicted acoustoelectric attenuation. This is different from the behavior observed for granular In/InO_x films,[17] in which the observed SAW attenuation was larger than the predicted acoustoelectric attenuation, and is due to the fact that the amorphous films are homogeneous over lengths which are much shorter than the SAW wavelength.

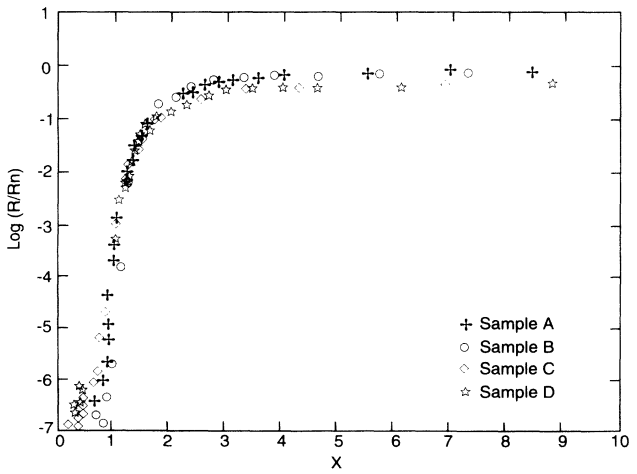

FIG. 6. $\ln(R/R_n)$ plotted as a function of the parameter X defined by Eq. (2).

The most interesting feature of these films is the presence of a "foot" in the attenuation data for samples *C*, *D*, and *E*. Looking at the normalized resistance and attenuation data, we see that the normalized curves coincide above $T \simeq T_c$, below which we see an excess attenuation. This behavior is different from that seen for the granular In/InO_x films[17] in that the deviation between the normalized attenuation and normalized resistance curves for the granular In/InO_x films occurred while the resistance was still nonzero. In addition, we see that the relative size of the foot seems to decrease as the normal-state sheet resistance of the sample increases. To verify this trend, sample *C* was annealed in order to decrease the normal-state resistance. The data for the anneals are given in Table II and the effects on the resistance and attenuation data are shown in Figs. 7 and 8. It is clear from the data in Fig. 8 that the relative size of the foot in the attenuation data decreases as the normal-state resistance increases.

Based on the observations made in the preceding paragraph, an explanation for the excess attenuation observed for $T < T_c$ is proposed in terms of the presence of vortex pairs. The bound vortex pairs, while not having an effect on the dc resistance, may indeed have an effect on the SAW attenuation. Early work done by Schenstrom *et al.*[18] on vortex-produced SAW attenuation suggested that the SAW attenuation produced by vortex pairs should be proportional to the fraction of the area of the film occupied by the normal cores of the vortices. One of the predictions of this model was that there would be a shift in temperature between the midpoints of the resistive and attenuation transitions. Clearly, as seen in Figs.

TABLE II. Anneal data on sample *C*.

Curve	Anneal time (h)	T_c (K)	T_{c0} (K)	R_n ($\Omega/\square$)	α_n (dB/cm)
a	no anneal	2.80	3.19	2660	5.97
b	30	2.91	3.21	1965	4.18
c	68.5	3.18	3.37	999	3.24

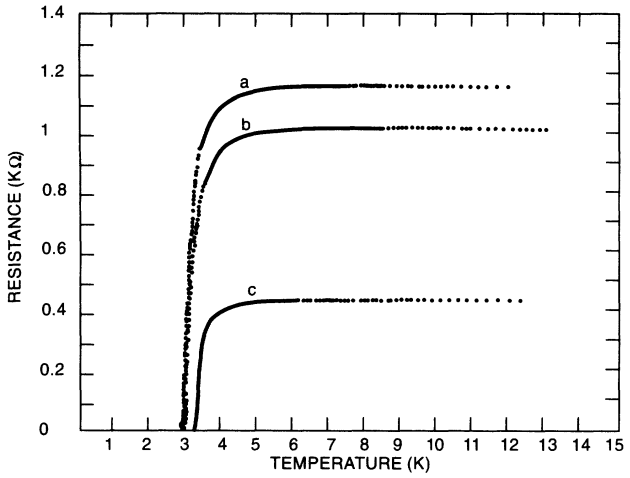

FIG. 7. Resistance data for sample C for different anneals: (a) no anneal, (b) first anneal, (c) second anneal.

1–5 this is not the case for the films that were studied. Thus, an alternative explanation is suggested.

The model that we propose for the vortex-produced attenuation is based on an extension of the work done by Halperin and Nelson[19] on the frequency dependent conductivity due to the presence of free vortices, which in turn is an application of the work done by Ambegaokar *et al.*[20] for the case of superconducting films. In their work, Halperin and Nelson considered the frequency dependent conductivity above T_c where all of the vortices are unbound. In our case, we are interested in the frequency dependent conductivity below T_c where all of the vortices are bound in pairs. According to Halperin and Nelson, the frequency dependent (two-dimensional) conductivity is related to the frequency dependent vortex "dielectric function," $\epsilon(\omega)$, according to

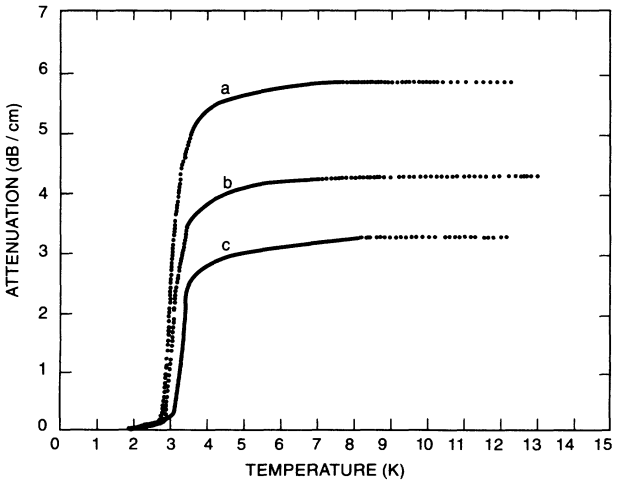

FIG. 8. SAW attenuation data corresponding to the resistance data of Fig. 7.

$$\sigma(\omega)=-\frac{n_0e^2}{i\omega m\epsilon(\omega)}\ , \tag{3}$$

where n_0 is the "bare" superelectron density, m is the electron mass and

$$\epsilon(\omega)=\epsilon_b+\frac{i\gamma}{\omega}\ . \tag{4}$$

In (4), ϵ_b is the contribution to $\epsilon(\omega)$ due to bound vortices and $i\gamma/\omega$ is the contribution due to free vortices. Since we are interested in the temperature region below T_c, we can neglect the second term in (4). Thus, (3) becomes

$$\sigma(\omega)=-\frac{n_0e^2}{i\omega m\epsilon_b}\ . \tag{5}$$

For our purposes, it will be convenient to rewrite (5) in terms of sheet resistance rather than conductivity

$$R(\omega,T<T_c)=\frac{\omega m}{n_0e^2}(\epsilon_b''-i\epsilon_b')\ , \tag{6}$$

where we have written $\epsilon_b=\epsilon_b'+i\epsilon_b''$. Since we are only interested in the real part of (6), we have

$$R(\omega,T<T_c)=\frac{\omega m\epsilon_b''}{n_0e^2}\ . \tag{7}$$

In order to evaluate (7) we must first know the functional form of $\epsilon_b''=\mathrm{Im}[\epsilon_b]$. This function has been studied by Ambegaokar *et al.*[20] for the case of a superfluid helium film and is given by

$$\epsilon_b''\simeq\frac{\pi}{4}\left|r\frac{d\tilde{\epsilon}(r)}{dr}\right|_{r=(14D/\omega)^{1/2}}\ , \tag{8}$$

where D is the vortex diffusion constant and $\tilde{\epsilon}(r)$ is a "length-dependent dielectric constant"[1,20] which was introduced into the Kosterlitz-Thouless theory to account for screening effects due to the presence of other bound vortex pairs. If the separation between the vortices is sufficiently large, then, for a superfluid helium film, we have

$$\tilde{\epsilon}(r)\simeq\tilde{\epsilon}_\infty\{1+\tfrac{1}{2}X(T)(r/a)^{-X(T)}\}\ . \tag{9}$$

In (9), a is a distance which is on the order of the interatomic distance and $X(T)$ is given by

$$X(T)=-4+\frac{2\pi h^2\rho_s(T)}{m^2k_BT}\ , \tag{10}$$

where $\rho_s(T)$ is the superfluid density. To apply Eqs. (8)–(10) to the case of a superconducting film, we replace $\rho_s(T)/t$, where t is the film thickness, by $\eta_s(T)$, the two-dimensional superconducting electron density, m by $2m$ and the quantity a by the Ginsburg-Landau coherence length ξ_{GL}.

For simplicity, we will consider the case when the temperature is just below T_c. In this case, the expression for $X(T)$ simplifies to[20]

$$X(T)\simeq b\left[1-\frac{T}{T_c}\right]^{1/2}, \tag{11}$$

where b is a nonuniversal constant assumed to be of order unity. Substituting (9) into (8) and evaluating the derivative in (8), we have

$$\epsilon_b\simeq\frac{\pi\tilde{\epsilon}_\infty}{2}\left\{\frac{X^2(T)(14D/\xi_{\rm GL}^2\omega)^{-X(T)/2}}{[2+X(T)(14D/\xi_{\rm GL}^2\omega)^{-X(T)/2}]^2}\right\}. \tag{12}$$

The vortex diffusion constant (D) is equal to $\mu k_B T$ where μ is the vortex mobility. The vortex mobility, in turn, can be related to the normal-state sheet resistance by[20]

$$\mu=\frac{2e^2\xi_{\rm GL}^2}{\pi h^2}R_n\ . \tag{13}$$

Under these substitutions, (12) becomes

$$\epsilon_b\simeq\frac{\pi\tilde{\epsilon}_\infty}{2}\left\{\frac{X^2(T)[E(T)R_n/R_c]^{-X(T)/2}}{\{2+X(T)[E(T)R_n/R_c]^{-X(T)/2}\}^2}\right\}, \tag{14}$$

where $E(T)=28k_BT/h\omega$ and $R_c=\pi h/e^2=1294\ \Omega/\Box$. Substitution of (14) into (7) yields the following expression for the frequency dependent, normalized resistance for T slightly less than T_c

$$\frac{R(\omega,T)}{R_n}\simeq\frac{\pi m\tilde{\epsilon}_\infty\omega}{2n_0e^2R_n}\left\{\frac{X^2(T)[E(T)R_n/R_c]^{-X(T)/2}}{\{2+X(T)[E(T)R_n/R_c]^{-X(T)/2}\}^2}\right\}, \tag{15}$$

Within this model, the attenuation due to vortices is being produced by the acoustoelectric effect and because of this, the normalized attenuation is equal to the normalized resistance. Thus, (15) gives us the normalized attenuation due to bound vortex pairs for temperatures just below T_c. All of the quantities in the prefactor of (15), except for n_0, are constant. Following Halperin and Nelson, we write $n_0=4d\alpha/\beta$ where α and β are, respectively, the coefficients of the $|\psi|^2$ and the $|\psi|^4$ terms in the expression for the Ginsburg-Landau free energy. We ignore the temperature dependence of β and write $\alpha=\alpha'(1-T/T_{c0})$. Under these assumptions, the expression for the normalized attenuation due to vortex pairs can be written as

$$\frac{\alpha(T<T_c)}{\alpha_n}\simeq A\frac{\{(1-T/T_c)/(1-T/T_{c0})\}\{28k_BTR_n/h\omega R_c\}^{-X(T)/2}}{\{2+X(T)[28k_BTR_n/h\omega R_c]^{-X(T)/2}\}^2}, \tag{16}$$

where

$$A=\frac{\pi\beta\tilde{\epsilon}_\infty m\omega}{8e^2\alpha' dR_n}, \tag{17}$$

and $X(T)$ is given by (11).

Equation (16) qualitatively explains the features seen in the observed attenuation data. First, (16) predicts that the attenuation due to bound vortex pairs is proportional to $R_n^{-m(T)}$, where $1\geq m(T)\geq\frac{1}{2}$. This would account for the fact that the relative size of the foot seen in the attenuation data decreases as the normal-state resistance increases. Second, we see that $\alpha/\alpha_n\to 0$ as $T\to 0$. Finally, we see that at $T=T_c$, $\alpha/\alpha_n=0$ as it should because at T_c all of the vortex pairs dissociate into free vortices and the contribution to the attenuation due to vortex pairs vanishes.

Figure 9 gives a graphical picture of the mechanisms involved in producing the SAW attenuation within the realm of the model just presented. In the temperature region $T_c<T<T_{c0}$, the SAW attenuation is acoustoelectrically produced by the presence of free vortices and is proportional to the flux-flow resistance of the free vortices. In the temperature region $T<T_c$ the attenuation is given by (16) and is being produced by the polarization of the bound vortex pairs due to the presence of the alternating currents associated with the surface wave. The reorientation of the bound pairs caused by the alternating currents of the SAW gives rise to the observed attenuation. In a real system, the SAW attenuation in the region near T_c would be represented (approximately) by the dashed

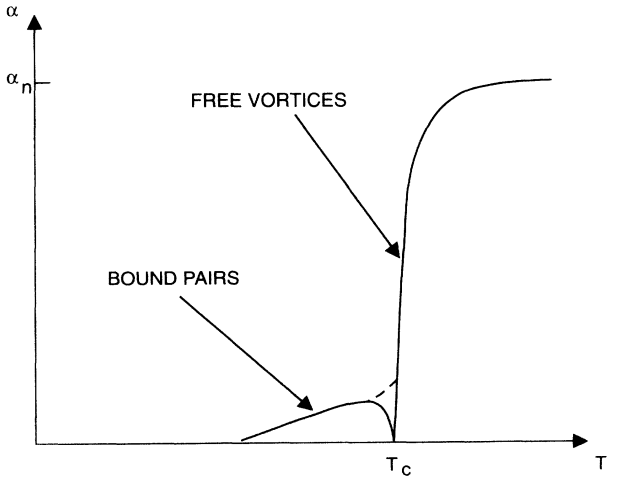

FIG. 9. Graphical representation of the SAW attenuation due to the presence of bound and free vortices.

curve in Fig. 9, since there will be some free vortices just below T_c and some vortex pairs just above T_c.

In Figs. 10(a)–10(e) we compare the normalized SAW attenuation data for samples C–E (including the annealed data for sample C) to the SAW attenuation predicted by (16). In evaluating (16), the constant A was taken to be a variable parameter because it contains quantities that are unknown and sample dependent. The value of A was determined by the best fit to the SAW attenuation data below T_c and was found to be equal to 2 for samples D and E, and 1 for sample C. As can be seen, the model that we have developed provides qualitative agreement with the experimental data, although the model predicts a more gradual decrease in attenuation than is observed. Two very important points must be kept in mind when comparing (16) to the experimental data. First, (16) is only really valid for temperatures close to T_c. We have clearly extended (16) beyond its range of validity in Figs. 10(a)–10(e). Attempts to redo the calculation for a wider range of temperature leads to an equation with too many undetermined parameters to easily compare to the experimental data. Second, we were limited by the temperature constraints of the cryogenic system used in this investigation. It may be that the minimum in attenuation is below the 1.5 K limit of the cryostat. If so, then this would affect the quantitative agreement between (16) and the experimental data. Keeping these two points in mind, the agreement between (16) and the experimental data is reasonable.

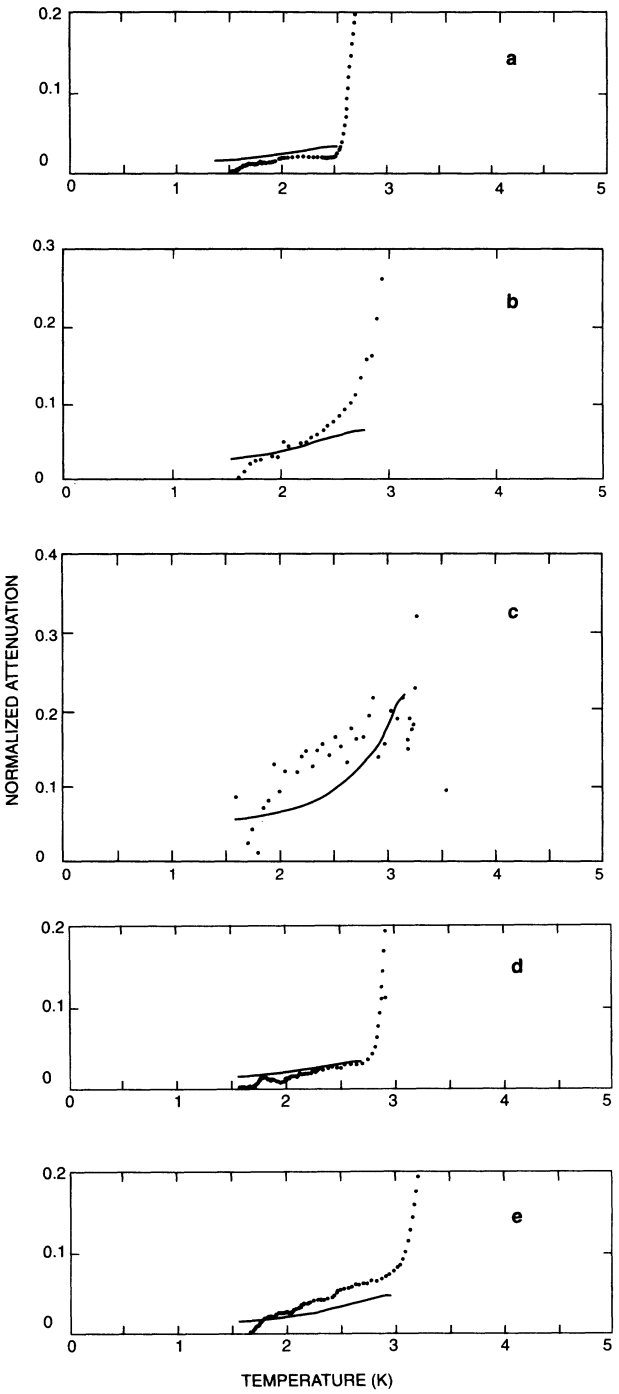

FIG. 10. Comparison of the SAW attenuation data for (a) sample C (points) to the prediction of the bound vortex model (solid curve) for $T < T_c$, (b) sample D (points) to the prediction of the bound vortex model (solid curve) for $T < T_c$, (c) sample E (points) to the prediction of the bound vortex model (solid curve) for $T < T_c$, (d) for the first anneal of sample C (points) to the prediction of the bound vortex model (solid curve) for $T < T_c$, (e) the second anneal of sample C (points) to the prediction of the bound vortex model (solid curve) for $T < T_c$.

CONCLUSION

Experimental data have been obtained on the dc resistance and SAW attenuation for five In/InO_x films. Although the primary focus of this investigation was on the study of the SAW attenuation, the resistance data were compared to the universality prediction of Minnhagen. It was found that the resistance data obtained on the In/InO_x films supports the predictions of Minnhagen.

As for the attenuation data, several observations were made. First, the normal-state attenuation of all of the films was very close to the predicted acoustoelectric attenuation, suggesting that the attenuation is acoustoelectrically produced. Second, three of the samples exhibited a "foot" in the attenuation data for temperatures less than the Kosterlitz-Thouless transition temperature. It is believed that this attenuation is being produced by the polarization of bound vortex pairs in the film. A model has been presented which suggests that two mechanisms are responsible for the SAW attenuation. Above T_c, the attenuation is proportional to the flux-flow resistance of the free vortices. Below T_c, the attenuation is being produced by the polarization of bound vortex pairs. This model provides qualitative agreement with the experimental data.

Finally, two of the samples (A and B) studied showed no appreciable foot in the attenuation data. These two samples were also the highest resistance samples which were studied. A simple analysis based upon the results of the model developed in this paper could account for the apparent lack of a foot in the attenuation data for these two samples. It was found that in the model presented here, the normalized attenuation was proportional to $R_n^{-m(T)}$ where $m(T)$ was between 1 and $\frac{1}{2}$. Using sample C as a comparison and assuming no sample-dependent

factors, the predicted normalized SAW attenuation for the foot for sample B should be between $\frac{1}{2}$ and $1/\sqrt{2}$ of that seen for sample C, and the foot for sample A should be between $\frac{1}{4}$ and $\frac{1}{2}$ of that seen for sample C. Such low values of attenuation could easily be masked by noise in the detection equipment. Also, the T_c's for samples A and B lie beyond the limits of the cryostat used in this investigation. A foot may indeed be present in these two films, but the limits of the experimental apparatus used in this investigation may be preventing us from seeing the bound vortex contribution in these samples below T_c.

ACKNOWLEDGMENT

The work at UWM was supported by the Office of Naval Research.

*Present address: AT&T Bell Laboratories, Naperville, IL 60566.

[1]J. M. Kosterlitz and D. J. Thouless, J. Phys. C **6**, 1181 (1973).
[2]M. R. Beasley, J. E. Mooij, and T. P. Orlando, Phys. Rev. Lett. **42**, 1165 (1979).
[3]A. T. Fiory, A. F. Hebard, and W. I. Glaberson, Phys. Rev. B **28**, 5075 (1983).
[4]K. Epstein, A. M. Goldman, and A. M. Kadin, Physica B+C **109&110B**, 2087 (1982).
[5]K. Epstein, A. M. Goldman, and A. M. Kadin, Phys. Rev. Lett. **47**, 534 (1981).
[6]A. M. Kadin, K. Epstein, and A. M. Goldman, Phys. Rev. B **27**, 6691 (1983).
[7]A. F. Hebard and A. T. Fiory, Phys. Rev. Lett. **50**, 1603 (1983).
[8]A. F. Hebard and A. T. Fiory, Physica B+C **109&110B**, 1637 (1982).
[9]A. F. Hebard and A. T. Fiory, Phys. Rev. Lett. **58**, 1131 (1987).
[10]H. Tejima, J. Schmidt, C. Figura, and M. Levy, *1983 IEEE Ultrasonics Symposium Proceedings,* edited by B. R. McAvoy (IEEE, New York, 1983), p. 1100.
[11]L. G. Aslamosov and A.I. Larkin, Fiz. Tverd. Tela (Leningrad) **10**, 1104 (1968) [Sov. Phys. Solid State **10**, 875 (1968)].
[12]H. P. Fredricksen, M. Levy, and J. Gavaler, Physica **107**, 113 (1981).
[13]K. A. Ingebrigtsen, J. Appl. Phys. **40**, 2681 (1969).
[14]K. A. Ingebrigtsen, J. Appl. Phys. **41**, 454 (1070).
[15]R. Adler, IEEE Trans. Sonics and Ultrason. **SU-18**, 115 (1971).
[16]P. Minnhagen, Phys. Rev. B **24**, 6758 (1981).
[17]J. Schmidt, M. Levy, and A. F. Lebard, Phys. Rev. B **43**, 505 (1991).
[18]A. Schenstrom, M. Levy, H. P. Fredricksen, and J. Gavaler, J. Phys. (Paris) Colloq. **46**, C10-703 (1985).
[19]B. I. Halperin and D. R. Nelson, J. Low Temp. Phys. **36**, 599 (1979).
[20]V. Ambegaokar, B. I. Halperin, D. R. Nelson, and E. Siggia, Phys. Rev. Lett. **40**, 783 (1978).